Research Article

Chemical Synthesis of Gadolinium Oxide Mediated Electrodes for Supercapacitor Application: Effect of Contact Angle

Dilip. K. Sahoo[1], Vaibhav. D. Patake[2*]

[1]Department of Physics, Shri Jagdishprasad Jhabarmal Tibrewala University, Vidyanagari, Jhunjhunu 333001, Rajasthan, India
[2]Department of Physics, Rani Channamma University, PB NH-4, Belagavi 591156, Karnataka, India
 E-mail: vdp.vaibhav@gmail.com

Abstract: Thin films of gadolinium oxide and gadolinium oxide-based electrodes were deposited on a stainless steel substrate employing the successive ionic layer adsorption and reaction (SILAR) method. The X-ray diffraction (XRD) study showed the formation of amorphous material on a substrate and the composition of the material was confirmed by the energy dispersive study (EDS). The water contact angle measurement showed the super-hydrophobic surface of the deposited material. The morphology showed gadolinium oxide resembled finger chip-type morphology while fungus-like and crocodile-back-like morphologies were observed for gadolinium oxide-copper oxide and gadolinium oxide-activated carbon (AC) composite correspondingly. The cyclic voltammetric measurement for supercapacitor application was carried out in a 0.2 M non-aqueous KCl electrolyte. It designated that the gadolinium oxide electrode with 94.22° contact angle had 106.25 $F \cdot g^{-1}$ specific capacitance. The super capacitance of electrodes was found to be depending on the contact angle concerning composition and morphology. The gadolinium oxide-copper oxide having 156.70° water contact angle possessed a specific capacitance of 52.66 $F \cdot g^{-1}$ while the gadolinium oxide-AC composite electrode carried 76.20 $F \cdot g^{-1}$ specific capacitance for 157.49° contact angle.

Keywords: chemical method, contact angle, gadolinium oxide, supercapacitor, thin film

1. Introduction

Supercapacitors have quickly become one of the most important electrochemical energy storage technologies due to their capacity to store electrical energy at a much bigger extent and rate than conventional capacitors and batteries. That's because supercapacitors are superior to those other two energy storage methods in terms of performance. A higher specific power density and lower internal resistance allow supercapacitors to store and distribute energy at much higher rates than more traditional energy storage devices [1-2]. A standard supercapacitor can be one of two varieties, each with its own unique energy storage mechanism [3]. The electrostatic charge accumulated at the electrode/electrolyte interface is the only source of capacitance in "electrical double layer capacitors" (EDLCs). This means that the electrode material's surface area has a significant impact on the capacitance. When it comes to the second type, a pseudo-capacitor, electro-active species are required to kick off fast reversible faradic reactions [4]. Due to advancements in nanotechnology, a wide variety of nanomaterials, nanostructures, nano-architectures, and nano-hybrids are now available options for use as supercapacitor electrodes [5-6]. It has opened up several hitherto untested avenues

for improving supercapacitor performance.

Carbon nanomaterials and their different hybrid topologies are commonly used in the fabrication of electrodes for high-performance supercapacitors. For instance, the high specific capacitance of 529.5 F·g^{-1} and 237.3 F·g^{-1} at the current density of 1 A·g^{-1} and 10 A·g^{-1}, and after 2,000 cycles have been reported for the electrodeposited MnO$_2$ on porous nickel foam [7]. Asymmetric supercapacitors with high energy density and high specific capacitance based on Ni-Co-Mn multiphase metal structure MOF showed a specific capacitance of 1,575 F·g^{-1} at 1 A·g^{-1} with remarkable rate capability and cycling stability [8]. There is a wide variety of carbon nanomaterials, including single-walled nanotubes (SWNTs), fullerene, multi-walled nanotubes (MWNTs), activated carbon (AC), graphene (Gr), graphene oxide (GO), reduced graphene oxide (rGO), and their hybrid architectures with polymers, metals, metal-organic frameworks (MOFs), and metal oxides [9-16]. Supercapacitor electrodes made from C-built materials, such as ACs and CNTs, are popular because of their many desirable physical and chemical properties [17]. They were regarded as researchable by experts due to their many enticing properties which comprised low price, a variety of shapes, ease of production, benign electrochemistry, regulated porosity, and electrocatalytically active sites for a variety of redox reactions. Activated carbon is typically understood to refer to a porous, three-dimensional and easily available carbon material with an irregular lattice structure that has high power and energy capabilities [18]. In addition to that vcarbon materials also had excellent specific capacitance derived from Chinese date [19] and efficient access of voltammetric charge in hybrid supercapacitor configured with potassium incorporated nano-graphitic structure derived from cotton (Gossypium arboreum) as negative and electrode [20]. The functionalized reduced graphene oxide/hexagonal boron nitride (rGO/h-BN) superlattice on the nickel foam electrode showed a high specific capacitance of ~1,300 F·g^{-1} [21].

Recently, rare earth (RE) material electrodes have also been attracted for the reason of psedo-capacitor behaviour since the oxidation state of the RE ion converted from (almost) 4$^+$ to a mixture of 3$^+$ and 4$^+$ [22, 23]. In the study of supercapacitor thin film electrodes of cerium oxide showed a specific capacitance of 78 F·g^{-1} and power density is 13.33 KW·Kg^{-1} in non-aqueous electrolytes [24]. Nanostructured lanthanum sulfide electrode with 46.9° contact angle exhibited a specific capacitance of 121.42 F·g^{-1} in 1 M Na$_2$SO$_4$ electrolyte [25] and enhanced up to 312 F·g^{-1} by making a composite with graphene oxide [26]. The films Gd$_2$O$_3$ prepared by pulse deposition and then POAP polymerization showed Specific capacitance, specific energy and specific power of 300 F·g^{-1}, 41.66 W·hkg^{-1} and 833.22 W·kg^{-1} respectively [27]. The egg-shaped gadolinium vanadate (GdVO$_4$) nanoparticles prepared using the simple soft chemical route presented specific capacitance to be 494, 480, 325, 190, 100 and 73 F·g^{-1} at current densities of 1, 2, 4, 6, 8, and 10 A·g^{-1} [28]. The multifunctional cubic lattice Gd$_2$O$_3$/CdO composite synthesized by the sol-gel method had a specific capacitance of 521 F·g^{-1} which is higher than the reported CdO and Gd$_2$O$_3$ oxides [29]. The gadolinia/nickel sulphide nanocomposite synthesized by the hydrothermal method offered a high specific capacitance of 354 F·g^{-1} at a constant current density of 0.5 A·g^{-1} [30]. A composite material of Gd$_2$O$_3$, Co$_3$O$_4$ and graphene on nickel foam had high specific capacitance of 3,616 F·g^{-1} with high-stability [31]. A Pulse electrosynthesised gadolinium oxide nanocomposite with polymer exhibited a specific capacitance of 300 F·g^{-1} for energy storage device [32]. A gadolinium oxide (Gd$_2$O$_3$) in Carbon Nanofiber Skeleton had 162.3 F·g^{-1} specific capacitance in supercapacitor application [33]. The as-synthesized electrode of Gd$_2$O$_3$/CuS possesses admirable rate performance (367 F·g^{-1}) and excellent cycle life [34]. These results may provide a new way to prepare composite electrodes for use in energy storage applications and promote other rare earth nanostructures.

The aim of this work was to synthesis and evaluate the performance of gadolinium oxide and gadolinium oxide mediated (by addition of other transition metal oxides and carbon base) electrode material for supercapacitor application. In this regard, the experiments were carried out to deposit the gadolinium oxide and composites with copper oxide and activated carbon by successive ionic layer adsorption reaction method on the stainless steel (SS) substrate. Further structural, and morphological studies were carried out by X-ray diffraction, scanning electron microscopy (SEM). The electrochemical characterizations were carried out in a non-aqueous KCl electrolyte. The performances of the electrodes were compared concerning material properties, morphologies along with water contact angles (WCA).

2. Experimental

The depositions of gadolinium oxide and its composites of thin films were carried out using the SILAR method

with both anionic and cationic precursors. The 0.01 M cationic solutions were prepared by AR grade gadolinium nitrate hexahydrate, copper sulphate and activated carbon (AC) in double distilled water separately. The composite thin films were prepared from the combination of equal concentrations of two different solutions mixed with constant stirring. The desired quantity of AR grade NaOH powder was immediately transferred and dissolved in double distilled water to form 0.01 M anionic precursor. The thin films were deposited on the stainless steel substrates by alternate dipping in anionic and cationic precursors. The thicknesses of films were determined by the gravimetric method [35] and calculated as the weight deposited by dividing the effective area of film ($g \cdot cm^{-2}$) on the substrate. The films were characterised using XRD techniques with Cu K_α radiation (λ = 1.5418 A°) on a Rigaku Ultima diffractometer in the 20-80° scanning angle range to obtain structural information. The films were scanned using JEOL JSM-6360 scanning electron microscope (SEM) at different magnifications to study the appearance of material deposit. The elemental existence was also confirmed at the same instant by the energy dispersive spectroscopy (EDS) unit. The hydrophilicity of the sample was determined using water contact angles (WCA) by contact angle metre (HO-IAD-CAM-01-Holmarc Opto-Mechatronics). The electrochemical behaviour of deposited materials for supercapacitor application was tested in 0.5 M KCl (aqueous and non-aqueous) electrolytes. The cyclic voltammetry (CV) experiments were carried out by using three electrode system where a saturated calomel electrode (SCE) was used as a reference, platinum as a counter and deposited films as a working electrode while the galvanostatic charge discharge (GCD) was carried out using two electrode system.

3. Result and discussion

3.1 Thin film formation

In the present experiment stainless steel (SS) grade 304 was used as substrates which constitutes a minimum of 66% iron, 17% chromium, and 8% nickel as per American standard stainless steel grade while the remaining part is composed of carbon, manganese, silicon, nitrogen, phosphorus, and sulfur. The substrate plays a crucial part in the deposition which should be clear of contaminants [36]. Before deposition substrates were mirror-polished with zero-grade polish paper and then washed with detergent then distilled water. After that substrates were cleaned ultrasonically and dried with hot air and methanol. In the deposition process of gadolinium oxide, the temperature of the anionic (OH^-) and cationic (Gd^{3+}) solutions were sustained at 300 K. In order to adsorb the gadolinium ions on the substrate, it was first submerged in a cationic precursor solution. After that, the substrate was washed in distilled water to remove any unbounded gadolinium ions. The substrate was introduced in the beaker continually through fixed time and is referred to as the adsorption time upheld in a cationic bath while the time in anionic bath is referred to as reaction time [37]. The gadolinium oxide (hydrated) film establishment was witnessed via iterating such a process involving the anionic precursor OH^- ions and Gd^{3+} ions. In one cycle of deposition, adsorption time and reaction time was 30 sec. and 10 sec. respectively while rinsing time was 10 sec. in distilled water in between the reactions. A layer formed after 50 cycles of deposition that was found to be suitable for further characterizations including electrochemical investigation for supercapacitors. Again same procedure was also used to formulate the composite electrode.

3.2 Characterizations of thin films

3.2.1 Thickness measurement and XRD studies

The gravimetric weight difference is a rapid and easy approach that can be used to measure film thickness (t) by using the formula [38].

$$t = \frac{m}{Ad} \tag{1}$$

where m is called the mass difference given as $m = m2 - m1$ ($m1$ = mass of the substrate before the deposition and $m2$ = mass of the substrate after the deposition). A is the area of the deposited film and d is the density of material in bulk form. Here it is noted that the density of the thin film is different than the bulk density and not applicable for porous and/or rough morphology so the final thickness was calculated as deposited weight by the deposited area and given in

terms of mg·cm^{-2} [35]. The film thickness of 0.4 mg·cm^{-2} was observed to be for gadolinium oxide film and found to be 0.6 mg·cm^{-2} for gadolinium oxide-copper oxide whereas 0.5 mg·cm^{-2} for gadolinium oxide-AC composite.

The thin films of gadolinium oxide and its composites were analysed by X-ray diffraction pattern (XRD) for structural information. Figure 1 provides (XRD) of as-deposited gadolinium oxide thin film for the instance. It showed the peaks originated from the substrates themselves may be because of low thickness or the formation of amorphous material [39, 40]. Similar kind of results were also noted (not shown) for gadolinium oxide composite films.
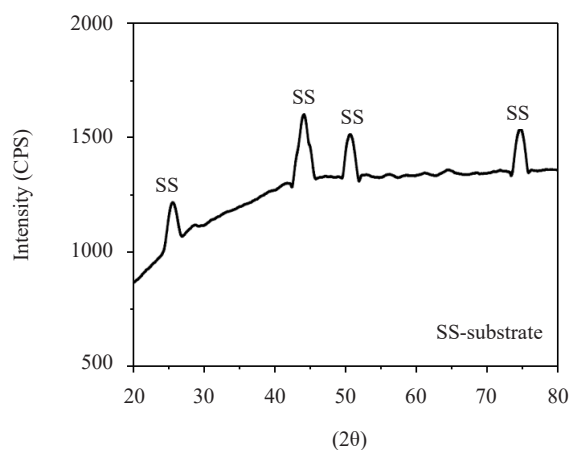
Figure 1. The XRD pattern of gadolinium oxide thin film

3.2.2 *Surface morphological and EDS study*

The morphology of gadolinium oxide thin films at different magnifications is displayed in Figure 2(a). It showed (inset) that grains on the surface were not well interconnected and formed cracked mud-type morphology at 3 kX while at higher magnification (10 kX) finger chips like morphology were observed. The cracked mud-type morphology may be observed because of the non-uniform or rough nature of the deposit formed by subaerial drying conditions at room temperature [41]. The elemental percentage of as-synthesized gadolinium oxide material was recorded by the EDS pattern (Figure 2(b)) which showed gadolinium is about 45% while oxygen covers 55% which concluded the formation of gadolinium oxide thin films on the substrate.

Figure 2(c) shows micrographs for as-deposited gadolinium oxide-copper oxide composite material having the cracked mud-like morphology of deposited material displayed in the inset at 3 kX while fungus-like morphology was observed at higher magnification. In the same way, the EDS pattern of the synthesized material is shown in Figure 2(d) which concluded the formation of gadolinium oxide and copper oxide composite material on the substrate. The other peaks in the spectrum arose because of the elemental composition of the stainless steel substrate which finds strain in the exact percentage of copper. Similarly, Figure 2(e) shows micrographs of gadolinium oxide-AC composite at 6 kX (inset) and 10 kX magnifications. It showed material covers almost the substrate surface observed at lower magnification while crocodile back-like morphology was observed at higher magnification. Likewise, the EDS pattern is shown in Figure 2(f) which concluded the formation of gadolinium oxide and activated carbon composite material. It showed the elemental percentage of gadolinium is about 18% and that of carbon 29% while the remaining 53% in the sample is covered by oxygen. Here it was observed the preparative conditions in the method were more favourable to depositing the gadolinium oxide than its composite. The morphologies observed from the SEM study are almost rough and porous which would be beneficial for the supercapacitor applications [24, 35, 39].
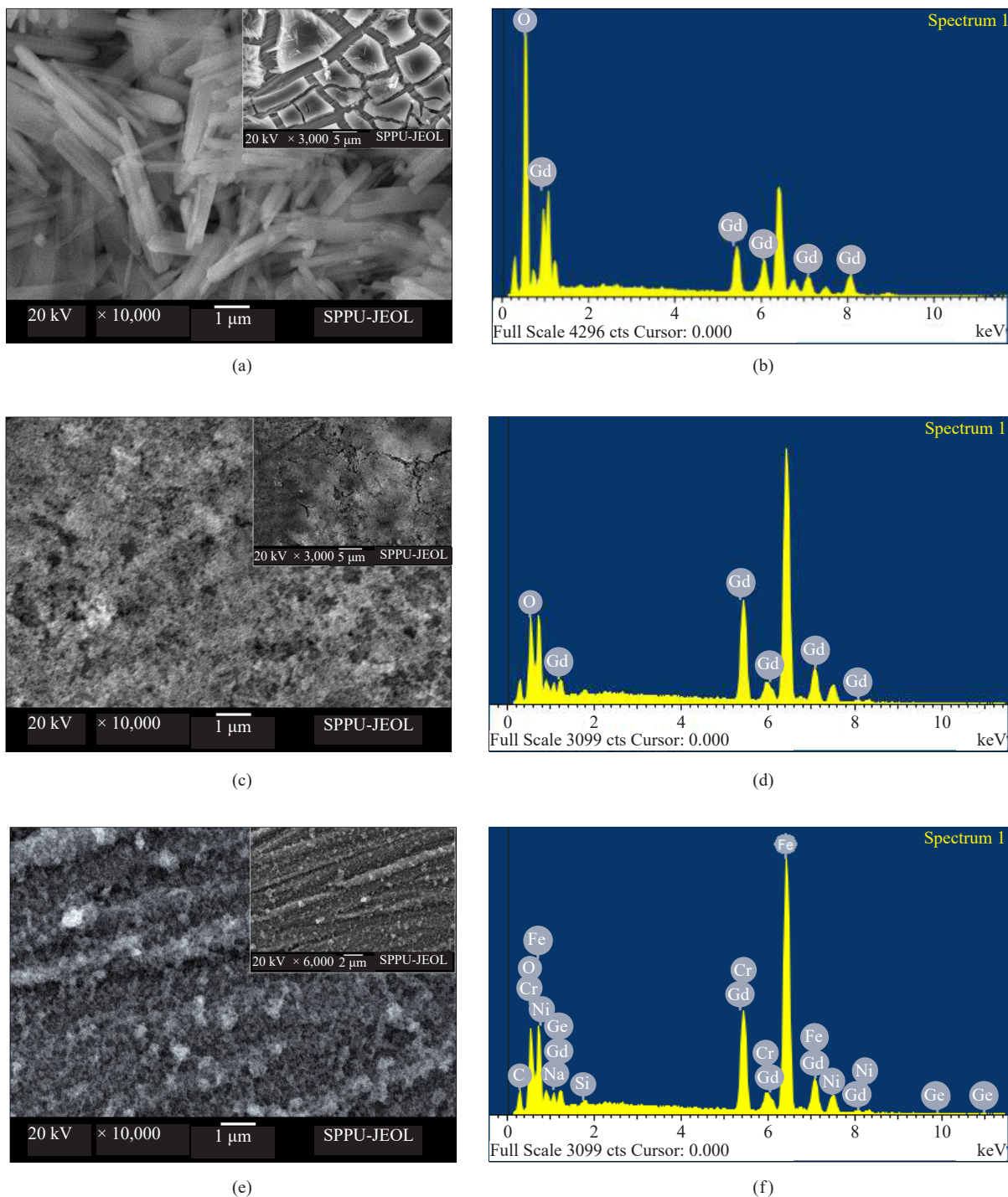
Figure 2. The morphology and EDS pattern of gadolinium oxide (a, b) gadolinium oxide-copper oxide (c, d) and gadolinium oxide-AC (e, f) films

3.2.3 *Water contact angle measurement*

The water contact angle of the film electrode is an important factor in achieving supercapacitance [42]. The average values of the WCA were recorded for the samples after the H_2O droplet got trapped over the surface. As shown in Figure 3(a) the gadolinium oxide film coating had a WCA of 94.22° on the left side and 93.83° on the right side concluding the hydrophobic character. On the other hand the gadolinium oxide-copper oxide coating in Figure 3(b) with WCA

of 156.70° on the left side but it had 152.92° on the right side. In the case of the gadolinium oxide-AC (Figure 3(c)) coating a water drop got caught at 157.20° and 155.49° on the left side and right side of the sample surface respectively. The contact angle measurement concluded that the film surface is turned from hydrophobic to super-hydrophobic. The increase in WCA may be observed because of the increase of oxide/carbon at the surface of gadolinium ions resulting in an increase of the hydrophobicity [22] resembling the effect of hydrocarbon adsorption reported by Preston et al. [43]. The hydrophilicity can also be controlled via organic material like fluorocarbon and graphene [44-46] and synthesised hydrophobic electrodes can be used as corrosion resistance in supercapacitor applications [44-50].

(a)

(b)

(c)
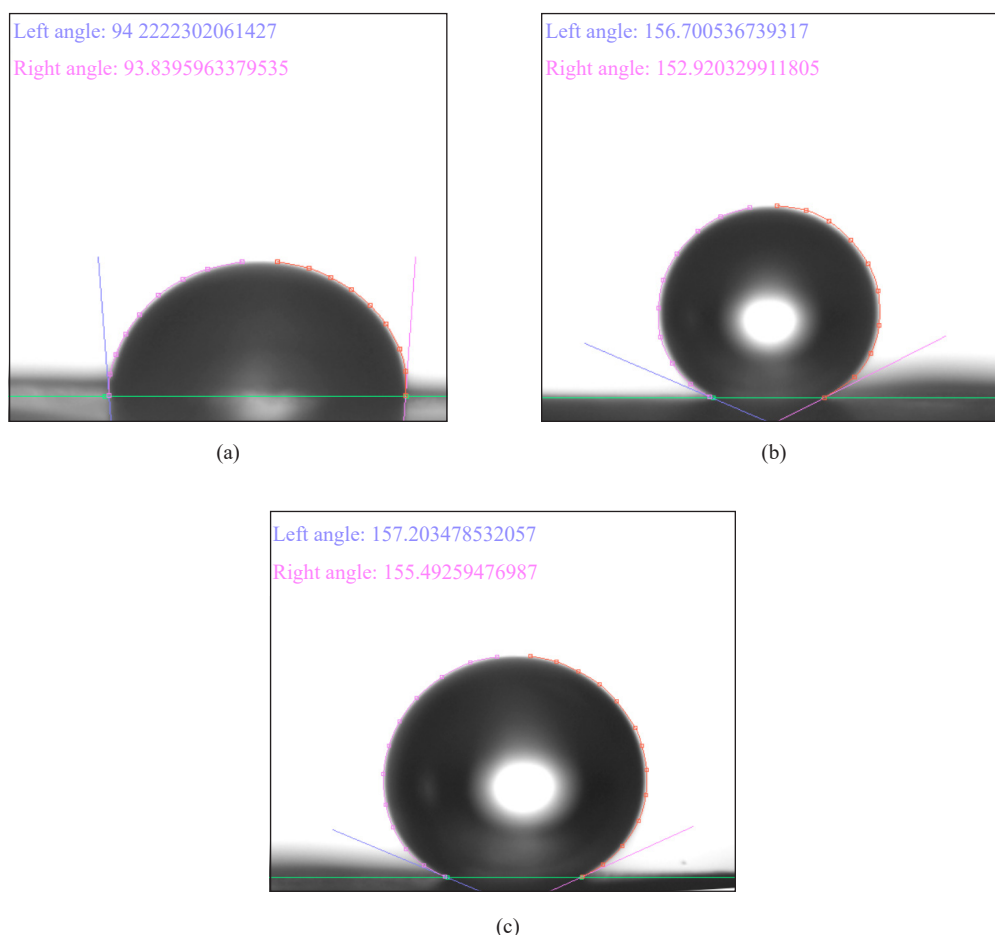
Figure 3. The water contact angle of the gadolinium oxide (a), gadolinium oxide-copper oxide (b) and gadolinium oxide-AC film (c)

3.2.4 *Performance of gadolinium oxide mediated electrode for supercapacitor application*

The purpose of this experiment was to understand the supercapacitor behaviour without the cyclic stability of a gadolinium oxide based electrodes in a non-aqueous and aqueous electrolyte similarly observed by Patake et al. for cerium oxide electrodes [24]. The gadolinium oxide mediated thin film electrodes were analysed in ~0.2 M KCl electrolytes both aqueous (double distilled water) and non-aqueous (dissolved in methanol) medium. During the cyclic scan gadolinium oxide electrode was not appropriate in aqueous electrolyte where as non-aqueous electrolyte was found suitable for further characterizations. The electrode showed redox peaks (not shown) and started to shift and completely disappeared after 10 cycles which confirmed the faradic natures of gadolinium oxide electrode. The effect on the supercapacitance performance of gadolinium oxide electrodes was investigated at different scan rates in non-aqueous 0.2 M KCl electrolyte. For instance, Figure 4(a) displayed the CV of a gadolinium oxide electrode at a 20 mVs^{-1} scan rate.

The figure showed the current response was not equally distributed in the positive and negative during oxidation and reduction which may be improved using symmetric electrodes [51]. The capacitance (C) and specific capacitance (C_s) were calculated using the following equations.

$$C = \frac{\int I}{V \times \left(\frac{dv}{dt}\right)}$$
(2)

$$C_S = \frac{C}{W}$$
(3)

Where, $\int I$- Integrated current within potential window V having $\left(\frac{dv}{dt}\right)$ scan rate and W is the weight of electrode material.

The cyclic voltammetric performances of gadolinium oxide were obtained at 20 mVs⁻¹, 50 mVs⁻¹, and 100 mVs⁻¹ scan rates (not shown) exhibited an increase in current using the scan rate. The gadolinium oxide electrode had a maximum specific capacitance of 106 F·g⁻¹ with a limiting value of 11.94 F·g⁻¹ at 20 mVs⁻¹ and 100 mVs⁻¹ scan rates respectively shown in Table 1. It indicates specific capacitance was decreased at the higher scan rate which strongly agrees with the literature [52]. The charge storage mechanisms hypothesized in processes may include the involvement of cations and electrons possessing the redox reactions as well as the surface adsorption/desorption process that contributes to the supercapacitance [53-55]. The value of the specific capacitance of electrodes was also found to be depending on the contact angle as shown in Figure 5. The maximum value of specific capacitance attained for gadolinium oxide electrode of nearly hydrophilic surface with 94.3° contact angle which may include more involvement of active species [42]. The outcome could be developed by introducing various types of substitutions and accepting various deposition methods [9-15].

Table 1. The supercapacitance study of gadolinium oxide mediated electrodes in 0.2 M non-aqueous KCl electrolyte

Sr. No	Scan rate (mVs⁻¹)	Interfacial capacitance (F·cm⁻²)			Specific capacitance (F·g⁻¹)		
		gadolinium oxide	gadolinium oxide-copper oxide	gadolinium oxide-AC	gadolinium oxide	gadolinium oxide-copper oxide	gadolinium oxide-AC
1	20	0.08	0.095	0.115	106.25	52.66	76.20
2	50	0.03	0.015	0.045	35.99	8.60	29.03
3	100	0.009	0.009	0.079	11.94	5.35	13.00

The inset of Figure 4(a) shows the galvanostatic charge-discharge (GCD) curve for gadolinium oxide electrode recorded using two electrode system throughout a potential range of (ΔE = 2 V/SCE) when the current density (ID) is 10 mA·cm⁻². The following equation 4 and 5 are used to calculate the energy density (ED) and power density (PD) of the electrodes by knowing the discharge time (TD) and the Ragone plot is shown in Figure 6 [20-21, 24-26]. The triangular-shaped curve by the GCD demonstrated the ideal supercapacitive nature of thin film electrodes with an energy density of 0.2546 Wh·Kg⁻¹ and power density of 8.33 KW·Kg⁻¹.
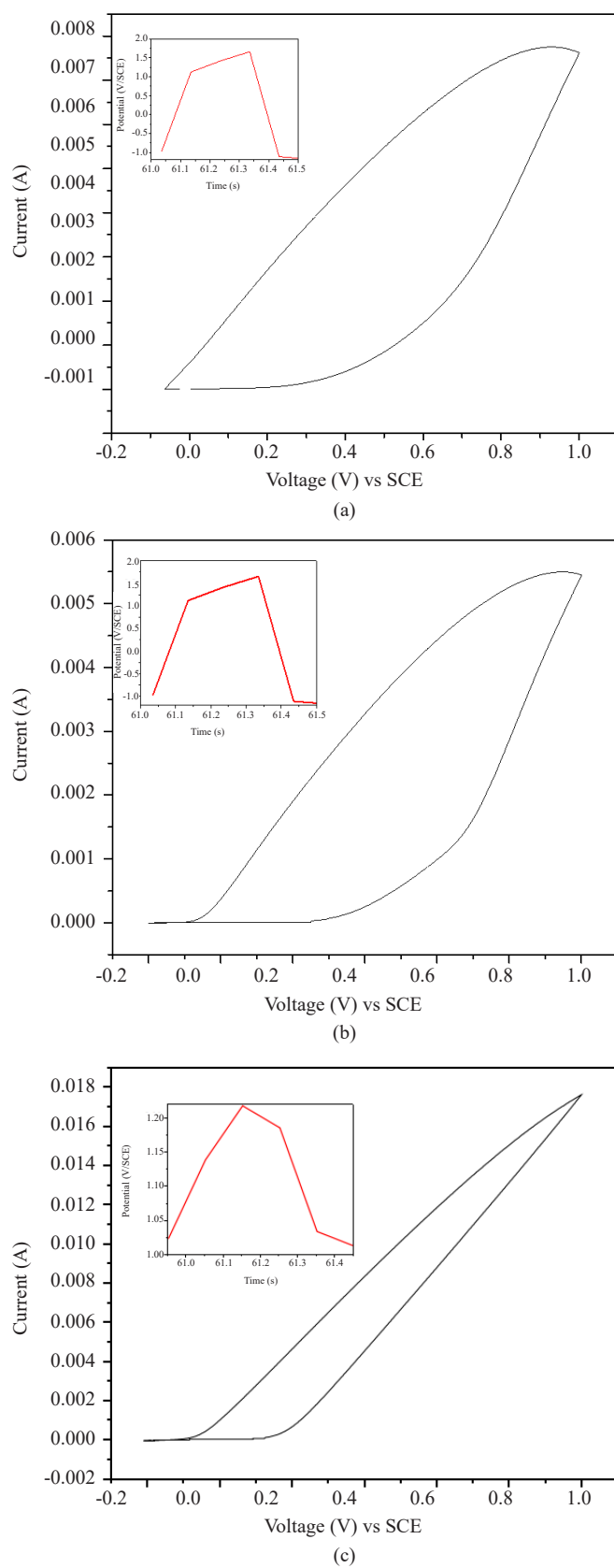
Figure 4. The cyclic voltammetry (CV) study of gadolinium oxide electrode thin film electrode (a), and gadolinium oxide-copper oxide composite electrode (b) and gadolinium oxide-AC composite electrode (c), in non-aqueous KCl electrolyte (20 mVs^{-1} scan rate) with GCD in the inset
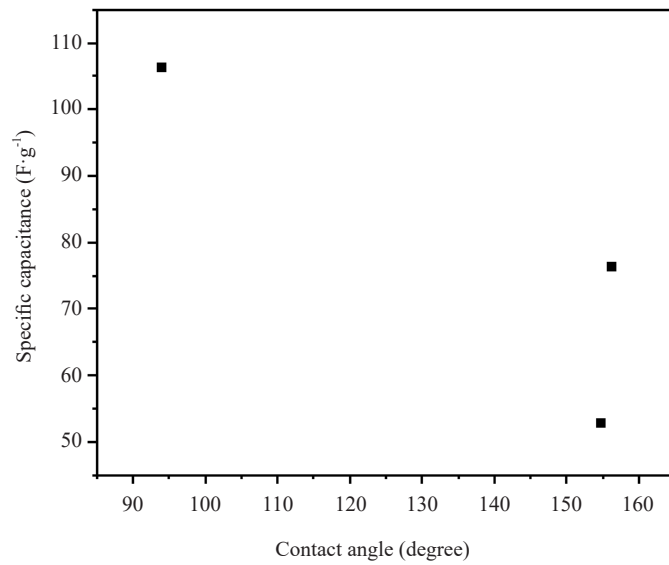
Figure 5. The graph of specific capacitance *Vs* contact angle
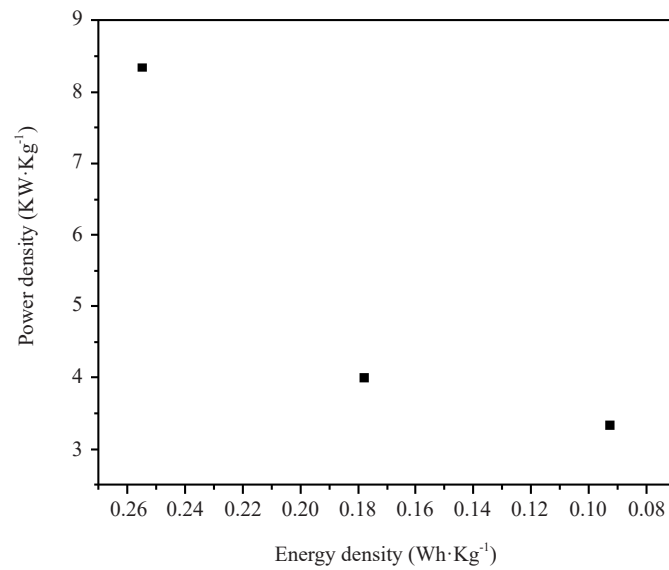
Figure6. The Ragone plot of gadolinium oxide and its composites

$$ED = \frac{0.5 \times C \times (\Delta E)^2}{3.6} \text{ where, } C = \frac{ID \times TD}{W \times \Delta E} \tag{4}$$

$$PD = \frac{ED \times 3,600}{TD} \tag{5}$$

The electrochemical behaviour of composite materials was also studied in a 0.2 M KCl non-aqueous electrolyte at 20 mVs^{-1}, 50 mVs^{-1} and 100 mVs^{-1} scan rates. The electrochemical responses of gadolinium oxide-copper oxides and gadolinium oxide-AC composite in 0.2 M KCl at 20 mVs^{-1} are shown in Figure 4(b) and Figure 4(c) respectively. The

triangular-shape nature of the GCD curve in the insets exhibited the ideal capacitive behaviour of thin film electrodes. The values of interfacial capacitance and specific capacitance were calculated using equations 2 and 3 and tabulated in Table 1. It can be seen that gadolinium oxide composites also displayed a negative correlation between the scan rates and capacitance values. The maximum value of specific capacitances achieved at 52.66 $F \cdot g^{-1}$ seems to be in contrast with earlier reports in supercapacitance enhancement by mixing material [26, 28]. It could happen because of a superhydrophobic surface (WCA 154.81°) which may restrict the species' involvement [22]. The gadolinium oxide-copper oxide composite electrodes possessed an energy density of 0.0925 $Wh \cdot Kg^{-1}$ with a power density of 3.33 $KW \cdot Kg^{-1}$ was obtained using equations 4 and 5. The value of super capacitance of the gadolinium oxide-AC composite electrode was observed to be 76.20 $F \cdot g^{-1}$ which was higher than the gadolinium oxide-copper oxide composite may contribute more capacitance from the double layer than the redox reactions. But this value is comparatively lower than gadolinium oxide in the present study and other AC-composite materials [56] might be since the retaining of higher contact angle 156.35° revealing superhydrophobic region. The results found inferior to gadolinium oxide (Gd_2O_3)/ carbon nanofiber composite [33] but superior to nickel-cobalt/AC composite which showed a specific capacitance of 59 $F \cdot g^{-1}$ in 1 M KCl [57]. The film under study possessed an energy density of 0.1776 $Wh \cdot Kg^{-1}$ and a power density of 3.99 $KW \cdot Kg^{-1}$ in 0.2 M non-aqueous KCl electrolyte. Figure 6 shows the Ragone plot of gadolinium oxide and composite. The maximum energy density is 0.2526 $KWh \cdot Kg^{-1}$ corresponding to a power density of 8.33 $W \cdot kg^{-1}$ achieved for gadolinium oxide. The energy density decreases to 0.0925 $KWh \cdot Kg^{-1}$ at a power density of 3.33 $W \cdot kg^{-1}$. For gadolinium oxide- copper oxide composite electrode. The energy density and corresponding power density were slightly increased up to 0.1776 $KWh \cdot Kg^{-1}$ and 3.99 $W \cdot kg^{-1}$ respectively in the case of the gadolinium oxide-AC composite electrode. It may happen because of the hydrophobic nature of electrodes which could follow the same relation with capacitance and contact angle as shown in Figure 5.

4. Conclusions

The binder-free gadolinium oxide and gadolinium oxide-based electrodes were deposited successfully by the SILAR method. The gadolinium oxide-based electrodes were found to unstable in aqueous (KCl) electrolyte and steady in non-aqueous (KCl) electrolyte with methanol as a solvent. It showed a specific capacitance of 106.25 $F \cdot g^{-1}$ for the gadolinium oxide electrode with a 94.22° contact angle however for the gadolinium oxide-copper oxide and gadolinium oxide-AC composite electrode the water contact angles of 156.70° and 157.49° with specific capacitances 52.66 $F \cdot g^{-1}$ and 76.20 $F \cdot g^{-1}$ respectively. The supercapacitance of the material contributes to redox reactions as well as a double layer. The contribution of a double layer would be found to be substantial for a larger contact angle. The specific capacitance of the materials was found to be dependent on material composition, morphology and also off the contact angle. The maximum value of energy density of 0.2546 $Wh \cdot Kg^{-1}$ and power density of 8.33 $KW \cdot Kg^{-1}$ was realized by pure gadolinium oxide film electrode.

Conflict of interest

On behalf of all authors involved in the manuscript, the corresponding author states that there is no conflict of interest.

References

[1] González A, Goikolea E, Barrena JA, Mysyk R. Review on supercapacitors: Technologies and materials. *Renewable and Sustainable Energy Reviews*. 2016; 58: 1189-1206.
[2] Zhao J, Burke AF. Review on supercapacitors: Technologies and performance evaluation. *Journal of Energy Chemistry*. 2021; 59: 276-291.
[3] Sharma K, Arora A, Tripathi SK. Review of supercapacitors: Materials and devices. *Journal of Energy Storage*. 2019; 21: 801-825.

[4]   Simon P, Gogotsi Y. Materials for electrochemical capacitors. *Nature Materials*. 2008; 7(11): 845-854.

[5]   Jalal NI, Ibrahim RI, Oudah MK. A review on supercapacitors: Types and components. *Journal of Physics: Conference Series*. 2021; 1973(1): 012015.

[6]   Yu A, Chabot V, Zhang J. *Electrochemical Supercapacitors for Energy Storage and Delivery: Fundamentals and Applications*. United Kingdom: Taylor & Francis; 2013.

[7]   Zhang M, Dai X, Zhang C, Fuan Y, Yang D, Li J. High specific capacitance of the electrodeposited MnO_2 on porous foam nickel soaked in alcohol and its dependence on precursor concentration. *Materials*. 2020; 13(1): 181.

[8]   Zhang B, Song S, Li W, Zheng L, Ma X. Asymmetric supercapacitors with high energy density and high specific capacitance based on Ni-Co-Mn multiphase metal structure MOF. *Ionics*. 2021; 27(8): 3553-3566.

[9]   Candelaria SL, Shao Y, Zhou W, Li X, Xiao J, Zhang JG, et al. Nanostructured carbon for energy storage and conversion. *Nano Energy*. 2012; 1(2): 195-220.

[10]   Suriyakumar S, Bhardwaj P, Grace AN, Stephan AM. Role of polymers in enhancing the performance of electrochemical supercapacitors: a review. *Batteries & Supercaps*. 2021; 4(4): 571-584.

[11]   Lokhande CD, Dubal DP, Joo OS. Metal oxide thin film based supercapacitors. *Current Applied Physics*. 2011; 11(3): 255-270.

[12]   Zhi M, Xiang C, Li J, Li M, Wu N. Nanostructured carbon-metal oxide composite electrodes for supercapacitors: a review. *Nanoscale*. 2013; 5(1): 72-88.

[13]   Lokhande VC, Lokhande AC, Lokhande CD, Kim JH, Ji T. Supercapacitive composite metal oxide electrodes formed with carbon, metal oxides and conducting polymers. *Journal of Alloys and Compounds*. 2016; 682: 381-403.

[14]   Muzaffar A, Ahamed MB, Deshmukh K, Thirumalai J. A review on recent advances in hybrid supercapacitors: Design, fabrication and applications. *Renewable and Sustainable Energy Reviews*. 2019; 101: 123-145.

[15]   Wang H, Feng H, Li J. Graphene and graphene-like layered transition metal dichalcogenides in energy conversion and storage. *Small*. 2014; 10(11): 2165-2181.

[16]   Patil PH, Kulkarni VV, Jadhav SA. An overview of recent advancements in conducting polymer-metal oxide nanocomposites for supercapacitor application. *Journal of Composites Science*. 2022; 6(12): 363.

[17]   Miao L, Song Z, Zhu D, Li L, Gan L, Liu M. Recent advances in carbon-based supercapacitors. *Materials Advances*. 2020; 1(5): 945-966.

[18]   Frackowiak E. Carbon materials for supercapacitor application. *Physical Chemistry Chemical Physics*. 2007; 9(15): 1774-1785.

[19]   Zhang YL, Sun C, Tang ZS. High specific capacitance and high energy density supercapacitor electrodes enabled by porous carbon with multilevel pores and self-doped heteroatoms derived from Chinese date. *Diamond and Related Materials*. 2019; 97: 107455.

[20]   Sanjit S, Milan J, Pranab S, Naresh CM, Tapas K. Efficient access of voltammetric charge in hybrid supercapacitor configured with potassium incorporated nanographitic structure derived from cotton (gossypium arboreum) as negative and $Ni(OH)_2$/rGO composite as positive electrode. *Industrial & Engineering Chemistry Research*. 2016; 55(42): 11074-11084.

[21]   Saha S, Samanta P, Murmu NC, Kim NH, Kuila T, Lee JH. Electrochemical functionalization and in-situ deposition of the SAA@ rGO/h-BN@ Ni electrode for supercapacitor applications. *Journal of Industrial and Engineering Chemistry*. 2017; 52: 321-330.

[22]   Külah E, Marot L, Steiner R, Romanyuk A, Jung T, Wäckerlin A, et al. Surface chemistry of rare-earth oxide surfaces at ambient conditions: reactions with water and hydrocarbons. *Scientific Reports*. 2017; 7(1): 43369.

[23]   Zhao H, Xia J, Yin D, Luo M, Yan C, Du Y. Rare earth incorporated electrode materials for advanced energy storage. *Coordination Chemistry Reviews*. 2019; 390: 32-49.

[24]   Sonar PA, Sanjeevagol SG, Manjanna J, Patake VD, Nitin S. Electrochemical behavior of cerium (III) hydroxide thin-film electrode in aqueous and non-aqueous electrolyte for supercapacitor applications. *Journal of Materials Science: Materials in Electronics*. 2022; 33(34): 25787-25795.

[25]   Ghogare TT, Pujari RB, Lokhande AC, Lokhande CD. Hydrothermal synthesis of nanostructured β-LaS_2 thin films. *Applied Physics A*. 2018; 124: 1-5.

[26]   Ghogare TT, Lokhande AC, Pujari RB, Lokhande CD. Lanthanum sulfide/graphene oxide composite thin films and their supercapacitor application. *SN Applied Sciences*. 2019; 1: 1-7.

[27]   Shiri HM, Ehsani A. Pulse electrosynthesis of novel wormlike gadolinium oxide nanostructure and its nanocomposite with conjugated electroactive polymer as a hybrid and high efficient electrode material for energy storage device. *Journal of Colloid and Interface Science*. 2016; 484: 70-76.

[28] He A, Feng L, Liu L, Peng J, Chen Y, Li X, et al. Design of novel egg-shaped GdVO$_4$ photocatalyst: a unique platform for the photocatalyst and supercapacitors applications. *Journal of Materials Science: Materials in Electronics*. 2020; 31: 13131-13140.

[29] Sivasamy R, Venugopal P, Mosquera E. Synthesis of Gd$_2$O$_3$/CdO composite by sol-gel method: Structural, morphological, optical, electrochemical and magnetic studies. *Vacuum*. 2020; 175: 109255.

[30] Dhanalakshmi S, Mathi Vathani A, Muthuraj V, Prithivikumaran N, Karuthapandian S. Mesoporous Gd$_2$O$_3$/NiS$_2$ microspheres: a novel electrode for energy storage applications. *Journal of Materials Science: Materials in Electronics*. 2020; 31(4): 3119-3129.

[31] Wang S, Lu S, Xu W, Li S, Meng J, Xin Y. Fabrication of a composite material of Gd$_2$O$_3$, Co$_3$O$_4$ and graphene on nickel foam for high-stability supercapacitors. *New Journal of Chemistry*. 2022; 46(25): 12184-12195.

[32] Shiri HM, Ehsani A. Pulse electrosynthesis of novel wormlike gadolinium oxide nanostructure and its nanocomposite with conjugated electroactive polymer as a hybrid and high efficient electrode material for energy storage device. *Journal of Colloid and Interface Science*. 2016; 484: 70-76.

[33] Aydın H, Üstün B, Kurtan Ü, Aslan A, Karakuş S. Incorporating Gadolinium Oxide (Gd$_2$O$_3$) as a rare earth metal oxide in carbon nanofiber skeleton for supercapacitor application. *ChemElectroChem*. 2024; 11(3): e202300585.

[34] Dhanalakshmi S, Babu IM, Karuthapandian S, Prithivikumaran N. Facile synthesis of mesoporous Gd$_2$O$_3$/CuS nanorods for high performance supercapacitors. *Materials Chemistry and Physics*. 2023; 309: 128355.

[35] Patake VD, Lokhande CD. Chemical synthesis of nano-porous ruthenium oxide (RuO$_2$) thin films for supercapacitor application. *Applied Surface Science*. 2008; 254(9): 2820-2824.

[36] Chang SK, Zainal Z, Tan KB, Yusof NA, Yusoff WMDW, Prabaharan SRS. Nickel-cobalt oxide/activated carbon composite electrodes for electrochemical capacitors. *Current Applied Physics*. 2012; 12(6): 1421-1428.

[37] Pathan HM, Lokhande CD. Deposition of metal chalcogenide thin films by successive ionic layer adsorption and reaction (SILAR) method. *Bulletin of Materials Science*. 2004; 27: 85-111.

[38] Pathan HM, Sankapal BR, Lokhande CD. Preparation of CdIn$_2$S$_4$ thin films by chemical method. *Indian Journal of Engineering and Materials Sciences*. 2001; 8(5): 271-274.

[39] Patake VD, Pawar SM, Shinde VR, Gujar TP, Lokhande CD. The growth mechanism and supercapacitor study of anodically deposited amorphous ruthenium oxide films. *Current Applied Physics*. 2010; 10(1): 99-103.

[40] Tüzemen EŞ, Eker S, Kavak H, Esen R. Dependence of film thickness on the structural and optical properties of ZnO thin films. *Applied Surface Science*. 2009; 255(12): 6195-6200.

[41] Yang SY, Man BY, Liu M, Chen CS, Gao XG, Wang CC, et al. Effect of substrate temperature on the morphology, structural and optical properties of Zn$_{1-x}$Co$_x$O thin films. *Applied Surface Science*. 2011; 257(9): 3856-3860.

[42] Patake VD, Lokhande CD, Joo OS. Electrodeposited ruthenium oxide thin films for supercapacitor: Effect of surface treatments. *Applied Surface Science*. 2009; 255(7): 4192-4196.

[43] Preston DJ, Miljkovic N, Sack J, Enright R, Queeney J, Wang EN. Effect of hydrocarbon adsorption on the wettability of rare earth oxide ceramics. *Applied Physics Letters*. 2014; 105(1): 011601.

[44] Yang C. Review of graphene supercapacitors and different modified graphene electrodes. *Smart Grid and Renewable Energy*. 2021; 12(1): 1-15.

[45] De Nicola F, Viola I, Tenuzzo LD, Rasch F, Lohe MR, Nia AS, et al. Wetting properties of graphene aerogels. *Scientific Reports*. 2020; 10(1): 1916.

[46] Zhang X, Wan S, Pu J, Wang L, Liu X. Highly hydrophobic and adhesive performance of graphene films. *Journal of Materials Chemistry*. 2011; 21(33): 12251-12258.

[47] Tan Y, Tang J, Zhao N, Qi F, Ouyang X. Effect of fluorocarbon polymers on hydrophobicity, wear resistance and corrosion resistance of epoxy resins. *Coatings*. 2023; 13(4): 685.

[48] Purkait T, Singh G, Kumar D, Singh M, Dey RS. High-performance flexible supercapacitors based on electrochemically tailored three-dimensional reduced graphene oxide networks. *Scientific Reports*. 2018; 8(1): 640.

[49] Chomkhuntod P, Iamprasertkun P, Chiochan P, Suktha P, Sawangphruk M. Scalable 18,650 aqueous-based supercapacitors using hydrophobicity concept of anti-corrosion graphite passivation layer. *Scientific Reports*. 2021; 11(1): 13082.

[50] Wang P, Wang Z, Zhang X, Liao Y, Duan W, Yue Y, et al. Stretchable superhydrophobic supercapacitor with excellent self-healing ability. *Energy & Fuels*. 2023; 37(7): 5567-5576.

[51] Cherusseri J, Kumar KS, Choudhary N, Nagaiah N, Jung Y, Roy T, et al. Novel mesoporous electrode materials for symmetric, asymmetric and hybrid supercapacitors. *Nanotechnology*. 2019; 30(20): 202001.

[52] Park BO, Lokhande CD, Park HS, Jung KD, Joo OS. Performance of supercapacitor with electrodeposited ruthenium oxide film electrodes-effect of film thickness. *Journal of Power Sources*. 2004; 134(1): 148-152.

[53] Murugan AV, Reddy MV, Campet G, Vijayamohanan K. Cyclic voltammetry, electrochemical impedance and ex situ X-ray diffraction studies of electrochemical insertion and deinsertion of lithium ion into nanostructured organic-inorganic poly (3, 4-ethylenedioxythiophene) based hybrids. *Journal of Electroanalytical Chemistry*. 2007; 603(2): 287-296.

[54] Dubal DP, Dhawale DS, Salunkhe RR, Lokhande CD. A novel chemical synthesis of Mn_3O_4 thin film and its stepwise conversion into birnessite MnO_2 during super capacitive studies. *Journal of Electroanalytical Chemistry*. 2010; 647(1): 60-65.

[55] Park HW, Kim T, Huh J, Kang M, Lee JE, Yoon H. Anisotropic growth control of polyaniline nanostructures and their morphology-dependent electrochemical characteristics. *Acs Nano*. 2012; 6(9): 7624-7633.

[56] Choi JR, Lee JW, Yang G, Heo YJ, Park SJ. Activated carbon/MnO_2 composites as electrode for high performance supercapacitors. *Catalysts*. 2020; 10(2): 256.

[57] Chang SK, Zainal Z, Tan KB, Yusof NA, Yusoff WM, Prabaharan SR. Nickel-cobalt oxide/activated carbon composite electrodes for electrochemical capacitors. *Current Applied Physics*. 2012; 12(6): 1421-1428.